Available online at www.sciencedirect.com
SCIENCE DIRECT®
Journal of Magnetic Resonance 174 (2005) 237–244
JMR Journal of Magnetic Resonance
www.elsevier.com/locate/jmr

Some aspects of quantitative 2D NMR

Harri Koskela [a,*], Ilkka Kilpeläinen [b], Sami Heikkinen [c]

[a] VERIFIN, University of Helsinki, P.O. Box 55, FIN-00014 Helsinki, Finland
[b] Department of Chemistry, University of Helsinki, P.O. Box 55, FIN-00014 Helsinki, Finland
[c] Helsinki Medical Imaging Center, University of Helsinki, P.O. Box 340, FIN-00029 HUS, Finland

Received 11 November 2004; revised 27 January 2005
Available online 11 March 2005

Abstract

We have studied the application of 2D HSQC for quantitative measurements and propose some improvements to the previously published Q-HSQC method. Application of CPMG-INEPT for polarization transfer period suppresses the evolution of J_{HH}, and thus corrects the shape of the cross-peaks. The better cross-peak shape makes phase correction and integration of the cross-peaks easier. Further, the ^{13}C resonance offset dependency can have a significant influence to the results. The offset effects can be compensated either by correcting results with a proper coefficient, or using 90° composite ^{13}C pulses in the pulse sequence. The results show that these modifications improve the applicability of 2D HSQC for quantitative analysis when studying molecules possessing large J_{HH} couplings and wide ^{13}C chemical shift range.

Keywords: 2D NMR; HSQC; CPMG; Quantification; Offset compensation

1. Introduction

NMR is a valuable structure elucidation tool for organic and biological molecules. Besides qualitative information, NMR can provide valuable quantitative information about a sample. A normal liquid state 1D ^1H NMR spectrum is commonly recognized as a reliable method for quantification. Other nuclei have also been utilized with one-dimensional experiments, both in liquids and solid state [1,2] As the complexity of samples increases, the resonance overlap forms a serious problem that easily degrades the accuracy of the analysis. Certain spectrum processing methods, like deconvolution, can help only to some extent. Hence a continuous pursuit has existed to find methods that can provide a good resolution while retaining reasonable quantitativity.

Two-dimensional heteronuclear shift-correlated methods give sufficient discrimination of resonances, as the correlation peaks are separated by chemical shifts of two nuclei. As these methods rely on polarization transfer through one-bond J coupling, the factors affecting quantitativity are far more complex than with a simple one-dimensional excitation–acquisition scheme. When the availability of substance is not an issue, X-nuclei detection can provide good resolution in the F_2 dimension, while resonances can be further discriminated by the proton chemical shift on the F_1 dimension [3,4]. This kind of approach, and some matters which have an influence on quantitativity, have been discussed in literature [5,6]. However, usually the amount of sample is restricted, so one has to rely on more sensitive methods, which exploit inverse detection.

In the previous study, HSQC [7] was modified to compensate $^1J_{CH}$-dependence of correlation peak volumes by selecting suitable polarization transfer values. The results indicated that this method, Q-HSQC [8], provided reliable quantitative information about lignin

* Corresponding author. Fax: +358 9 191 50437.
E-mail address: Harri.Koskela@oulu.fi (H. Koskela).

1090-7807/$ - see front matter © 2005 Elsevier Inc. All rights reserved.
doi:10.1016/j.jmr.2005.02.002

samples. It was also recognized, that if a proton has many J_{HH} couplings, this coupling evolution during polarization transfer periods could distort the line shape of the correlation peak, thus compromising the accuracy of result. In the current study we show that it is possible to avoid the influence of the J_{HH} couplings by replacing the polarization transfer steps with CPMG-type sequences. Further, we also show that the offset effects of the pulses on the heteronucleus (^{13}C) channel can be a major source of error. However, these effects can easily be accounted for, either by using suitable correction factors, or using 90° composite ^{13}C pulses in the pulse sequence.

2. Experimental methods

CPMG-INEPT polarization transfer period has been utilized in several studies [9–11]. Rapid repetition of simultaneous 180° pulses on proton and carbon channels in CPMG-INEPT suppresses the evolution of proton–proton couplings while the evolution of J_{CH} is still active. Thus, we have studied the suitability of CPMG-INEPT to replace the constant-time INEPT periods in Q-HSQC. It appears that the current approach, quantitative CPMG-adjusted heteronuclear single quantum coherence (Q-CAHSQC, Fig. 1), effectively avoids the J_{HH} evolution problems of the original experiment. The XY-16 sequence [12] is preferred over the normal 180° pulse train with single pulse phase, as the former preserves magnetization on all Cartesian axes.

In Q-HSQC [8], four acquisitions with different polarization transfer times were recorded per spectrum to give uniform intensity response over the wide range of $^{1}J_{CH}$ values. These polarization transfer times, Δ-values, were iteratively optimized for the $^{1}J_{CH}$-range of 115–190 Hz, and the best values were $\Delta_i = 2.94$, 2.94, 2.94, and 5.92 ms. The constant-time variant of CPMG-INEPT was constructed by introducing a continuous XY-16 sequence pulsing on proton channel with total time of Δ_{max}, which stands for the largest Δ-value (5.92 ms) while on carbon channel the XY-16 sequence was on for the time period of Δ_i. In practice this was carried out by setting the inter-pulse delay τ of XY-16 to 92.5 μs, so that the total duration of inter-pulse delays of two consecutive XY-16 sequence loops would be the required 5.92 ms. The value of τ was short enough to satisfy the condition $\tau < 1/(2\ \Delta\nu_{max})$, which is required for proper J_{HH} suppression [13–15]. The Δ-variation was then accomplished by introducing XY-16 simultaneously on carbon channel either during both of XY-16 periods ($\Delta = 5.92$ ms), or only during the second XY-16 period ($\Delta = 2.94$ ms).

We have also noticed that the wide chemical shift dispersion of the ^{13}C nuclei introduce some problems for the quantitativity of Q-HSQC, i.e., the response of the experiment is dependent on the chemical shift of the particular group in question. Therefore, the ^{13}C-channel off-resonance effects were compensated by modifying the sequence with composite pulses (Fig. 1C) The first 90° ^{13}C pulse in subsection II should deliver carbon magnetization transfer $z \rightarrow -y$ as efficiently and as purely as possible. Freeman et al. [16] have reported a 90° composite pulse that apply the "reversed rotation pulse" concept. It has good phase and offset properties on wide range of chemical shifts, and thus is excellent for the current task. The second 90° ^{13}C pulse needs to transfer magnetization $y \rightarrow z$ likewise as efficiently as possible. The aforementioned composite pulse is not suitable for this transfer, so it was replaced with a 90° composite pulse introduced by Tycko et al. [17]. It has a slightly less efficient offset compensation, but it delivers the magnetization transfer without significant phase distortion. The last carbon pulse in scrutiny in subsection II is the 180° pulse used for refocusing the chemical shift and heteronuclear coupling evolution during the coherence selection gradient. While a proper composite pulse could be applied to the task, the most effective way from the point of offset compensation is to omit this pulse, and embed the gradient pulse to t_1 evolution period (Fig. 1C, II′). Naturally, this approach causes significant phasing difficulties on F_1 axis due to the missing acquisition points at the beginning of t_1 evolution period. Fortunately, this can be compensated by using backward linear prediction to calculate these points. The amount of needed points can be calculated by dividing the delay δ with the duration of t_1 evolution increment. The δ can be adjusted to be an exact multiple of t_1 increment to make the phasing easier after linear prediction.

3. Results and discussion

A sample of strychnine was chosen for testing of the pulse sequences, as it is a very challenging molecule from the point of quantification. It bears a complex network of J_{HH} couplings, and additionally, it has a large chemical shift range of both proton and carbon resonances. Q-HSQC and Q-CAHSQC spectra of strychnine were recorded to estimate the effect of J_{HH} coupling(s) on the cross-peak shape and volume and thus to the quantitativity. As the polarization transfer period is quite long, the J_{HH} coupling evolution can twist the shape of cross-peak. This is clearly visible on F_2-projections of cross-peaks of geminal protons bearing large J_{HH} couplings (Fig. 2). The twisted cross-peak shape that can be seen on Q-HSQC spectrum places obvious difficulties to the integration, and can introduce a source of error to the results. In order to investigate the quantitativity, the positive intensities of cross-peaks were integrated, and the results were calibrated relative to the integral of H-4, which was set to 1.0 (Fig. 3). The

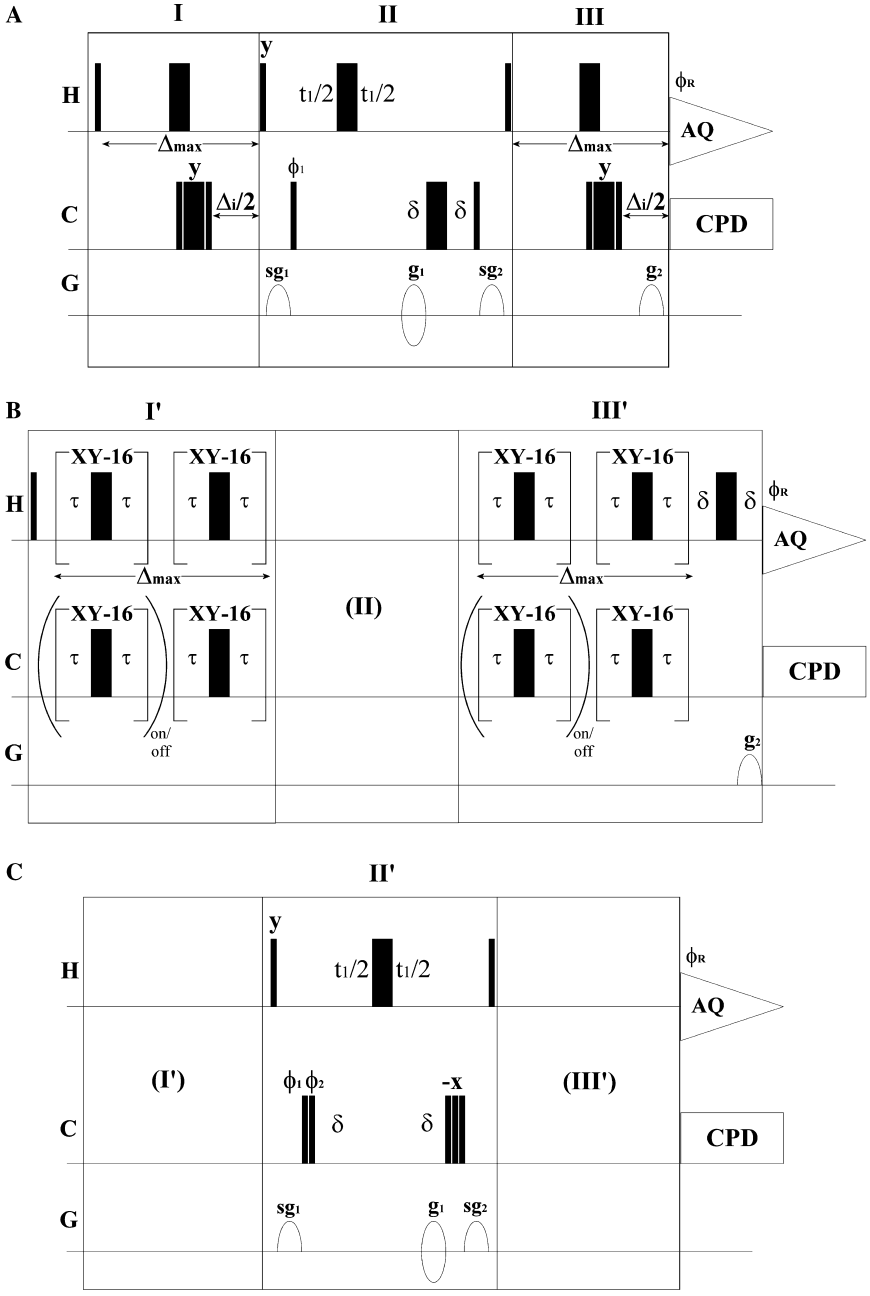

Fig. 1. The pulse sequences used during the study; Q-HSQC (A), Q-CAHSQC (B), composite pulse compensated Q-CAHSQC (C). The pulse sequences were divided into three subsections as shown. For the Q-CAHSQC (B) the polarization transfer periods I and III were replaced with constant-time CPMG-INEPT, while the evolution period II was kept the same. Additionally, for composite pulse compensated Q-CAHSQC (C) the evolution period II was also replaced to employ 90° composite pulses for carbon channel. The gradient selection of coherence was embedded into the t_1 evolution period. Backward linear prediction was then used to compensate the acquisition points for the duration δ. Narrow and thick bars represent the 90° and 180° RF pulses, respectively. The 90° pulse durations were 7.22 μs for ^{1}H and 12.70 μs for ^{13}C. Two different 90° composite pulses were utilized in subsection II′; the first was $360(\phi_1) - 270(\phi_2) - \delta'$, where δ' was 2* PW90(^{13}C)/π [16]. The second was $285(x) - 320(-x) - 25(x)$ [17]. Phase cycles were: $\phi_1 = \{x, -x\}$, $\phi_2 = \{-x, x\}$, and $\phi_R = \{x, -x\}$. The delays Δ_i were {2.94, 2.94, 2.94, and 5.92 ms}, and Δ_{max} was 5.92 ms. The XY-16 consist of 16 of 180° pulses with phases {x, y, x, y, y, x, y, x, $-x$, $-y$, $-x$, $-y$, $-y$, $-x$, $-y$, $-x$}, and 32 of τ-delays. The delay τ was set to 92.5 μs, so that the total duration of τ-delays for two consecutive XY-16 loops equals Δ_{max}. Total duration of τ-delays for one XY-16 loop is then 2.96 ms, which is close enough to the needed 2.92 ms. Thus, the Δ_i-variation was accomplished by turning the pulsing of the first XY-16 sequence on ^{13}C channel either *on* or *off* in the following way: $\Delta_{i(\text{CPMG-INEPT})} = \{off, off, off, on\}$. The pulsed field gradients are represented by half-ellipses. The PFG duration was 1 ms, with recovery delay of 100 μs, giving the delay δ a duration of 1.1 ms. The applied PFG strengths were: $g_1 = 48$ G/cm and $g_2 = 12$ G/cm, and the corresponding spoiler PFG strengths were $sg_1 = 54$ G/cm and $sg_2 = 44$ G/cm. For every increment of t_1, two-step phase cycle was conducted per every polarization transfer value of Δ_i, and the same was done with changed polarity of g_1 to carry out the gradient-based echo-anti-echo quadrature detection in the F_1-dimension. The axial peak displacement is achieved with the states-TPPI method by inverting the phases ϕ_1, ϕ_2 and ϕ_R on every second increment of t_1. The composite pulse decoupling was accomplished with GARP-1 on ^{13}C channel during acquisition.

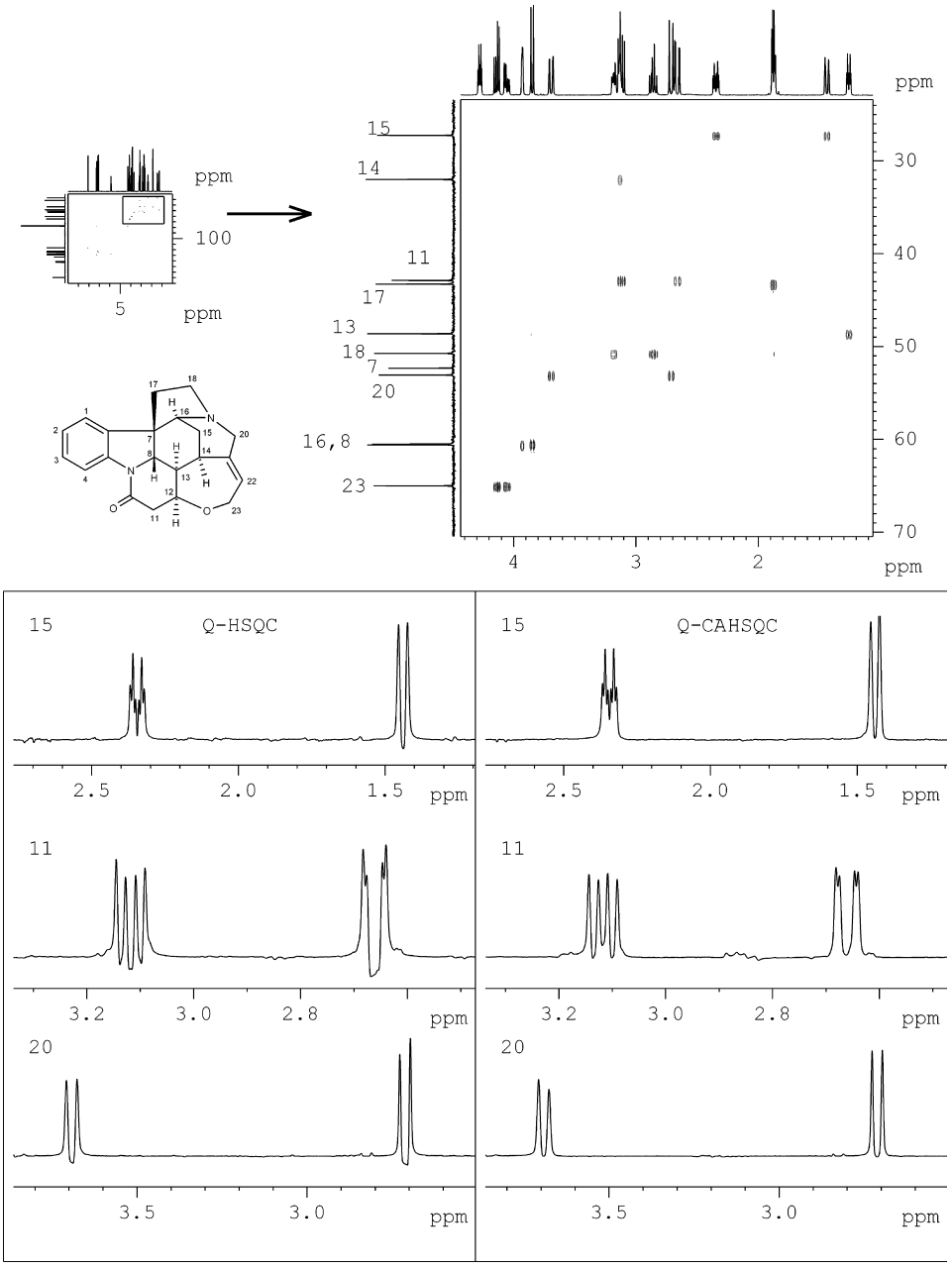

Fig. 2. F_2-projections from Q-HSQC and Q-CAHSQC spectra of strychnine at correlation peaks bearing large geminal J_{HH} couplings. All the spectra were recorded at 300 K with Bruker DRX 500 spectrometer equipped with 5 mm broad-band inverse probe with z-gradient. All spectral processing was performed with Bruker XWinNMR 3.0 software. The strychnine sample was prepared to 5 mm NMR tube by dissolving 60 mg strychnine to 0.5 ml $CDCl_3$. The 2D spectra were recorded using spectral widths of 10 and 200 ppm for ^1H (F_2) and ^{13}C (F_1) dimension, respectively. The carriage frequencies were at 5 and 100 ppm for ^1H and ^{13}C channel, respectively. A two-step phase cycle was employed (cf. Fig. 1) with four Δ-values, giving a total of 8 scans per transient. The number of dummy scans was 64. The repetition rate was set to 15.8 s to equal five times the longest $T_1(^1H)$ of strychnine (H-4). A total of 4k (F_2) × 400 (F_1) data points were recorded for a spectrum, giving a total acquisition time of 16 h 5 min. The spectra were weighted with squared sine bell function for both dimensions prior to Fourier transform. The final data matrix size after Fourier transform was 16k × 1k to ensure a good digital resolution. The spectra were integrated using positive intensity mode.

H-4 was chosen to be the reference, as it has the longest $T_1(^1H)$, and C-4 has the smallest ^{13}C offset. The integrals of e.g., H-11a and H-11b were 0.586 and 0.650, respectively, which indicates 9.8% difference in values. The Q-CAHSQC suppress J_{HH} evolution during polarization transfer steps, and the cross-peak shape is absorptive resulting much easier phasing of the 2D spectra, and the integration will be much easier to execute. Consequently, integrals of corresponding H-11a and H-11b cross-peaks show slight improvement giving 0.635 and 0.613, respectively, and the difference of values has diminished to 3.5%.

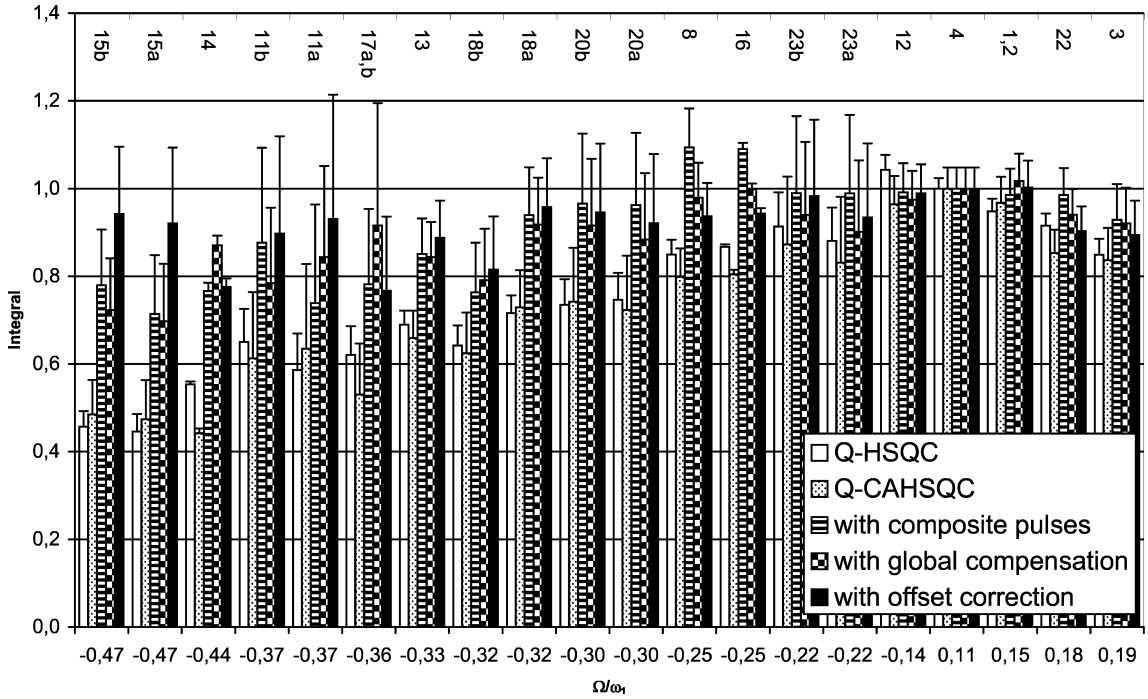

Fig. 3. Calibrated integration results from 2D experiments (Q-HSQC, Q-CAHSQC, Q-CAHSQC with composite pulse compensation and Q-CAHSQC after offset correction) of strychnine. The results are plotted against relative offset Ω/ω_1, where Ω is absolute ^{13}C offset in radians, and ω_1 ($=\gamma B_1$) is the ^{13}C RF field strength in radians. The integrals were calibrated against H-4, which was set to 1.0. Cross-peaks of H-1 and H-2 were integrated as one, and the value was divided by two. The value of H-17a,b was also divided by two. Positive error bars show the integral value after compensation of J_{HH} evolution for Q-HSQC and J_{HH} polarization transfer due to isotropic mixing for Q-CAHSQC.

Although the J_{HH} coupling evolution is suppressed during the CPMG-INEPT, a closely spaced 180° pulse train can erect an another interaction between protons; the isotropic mixing [18]. In theory, the intensity of cross-peak can be attenuated by a factor:

$$\prod_{i=1}^{k}\left(\frac{1}{2}(1+\cos(2\pi J_{\mathrm{HH}i}\Delta_{\max}))\right)^2. \quad (1)$$

This corresponds to a square of the attenuation that J_{HH} evolution in Q-HSQC can affect [8] to cross-peak integrals. Although the XY-16 sequence used during polarization transfer periods is not very effective in respect of homonuclear Hartmann–Hahn transfer, the attenuation level due to isotropic mixing was calculated from the actual J_{HH} constants. Corresponding error bars are included to the Fig. 3. Likewise, the attenuation due to J_{HH} evolution during Q-HSQC are calculated, as shown in Fig. 3. The results indicate that the J_{HH} contribution to cross-peak intensities can be quite remarkable if the cross-peak bears large proton–proton couplings, i.e., geminal coupling. For example, theoretical calculations express as much as 23% larger integral for H-11a in Q-CAHSQC, if attenuation due to isotropic mixing takes full effect. However, the integrals of H-11a and H-11b are for both methods about 40% lower than the integral of reference cross-peak H-4. The polarization transfer through J_{HH} evolution or isotropic mixing cannot explain this deviation in intensities. In fact, almost all of the integration results remain below 1.0 even with J_{HH} compensation (cf. Fig. 3). The deviation between the integrals shows a trend when they are plotted as a function of the carbon resonance offset. As expected, the wide chemical shift range of carbons will deliver substantial resonance offset effects with limited RF strength available. In the original Q-HSQC, the resonance offset compensation was applied on INEPT for inversion 180° carbon pulses. The simulations with Bloch module of Bruker NMR-SIM indicates, that XY-16 sequence itself has also quite good offset compensation (Fig. 4). So when bearing in mind that the offset compensation for XY-16 was practically flawless within band $\pm 0.5\ \gamma B_1$ (cf. Fig. 4), the highest-field carbon, (C-15), with offset of -9147 Hz should not experience any intensity degradation due to offset effects with $\gamma B_1 = 19.6$ kHz on ^{13}C channel. Thus, the main influence on the integrals is caused by 90° RF pulses during subsection II (cf. Fig. 1).

A way to compensate this offset dependency is to take it into account by multiplying the integration results with a correction factor (coefficient) that can be easily measured experimentally. The resonance offset profile was determined experimentally by recording a series of 1D Q-CAHSQC spectra from methanol in MeOH-d4. The offset of every ^{13}C pulse was varied about the

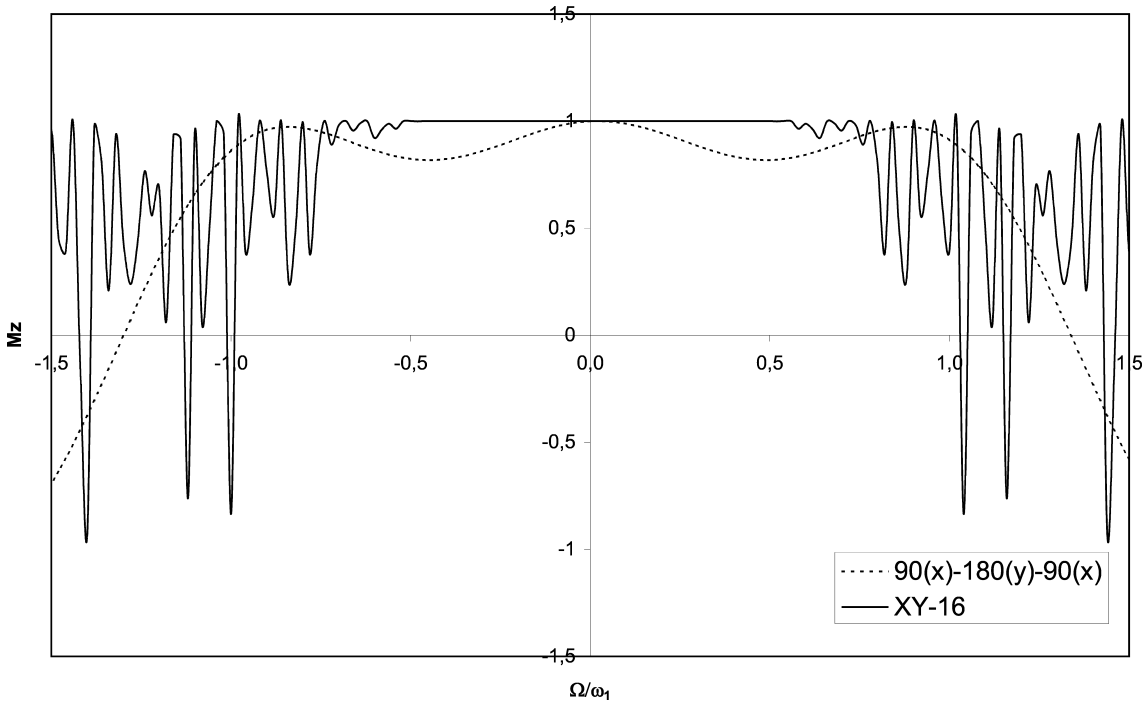

Fig. 4. The z-magnetization projections for XY-16 and $90(x) - 180(y) - 90(x)$ composite pulse. The results are plotted against relative offset Ω/ω_1, where Ω is absolute offset, and ω_1 ($=\gamma B_1$) is the RF field strength. The profiles were simulated with Bloch module of Bruker NMR-SIM software using 20 kHz for γB_1 strength. The inter-pulse delay τ for XY-16 was set to 100 μs.

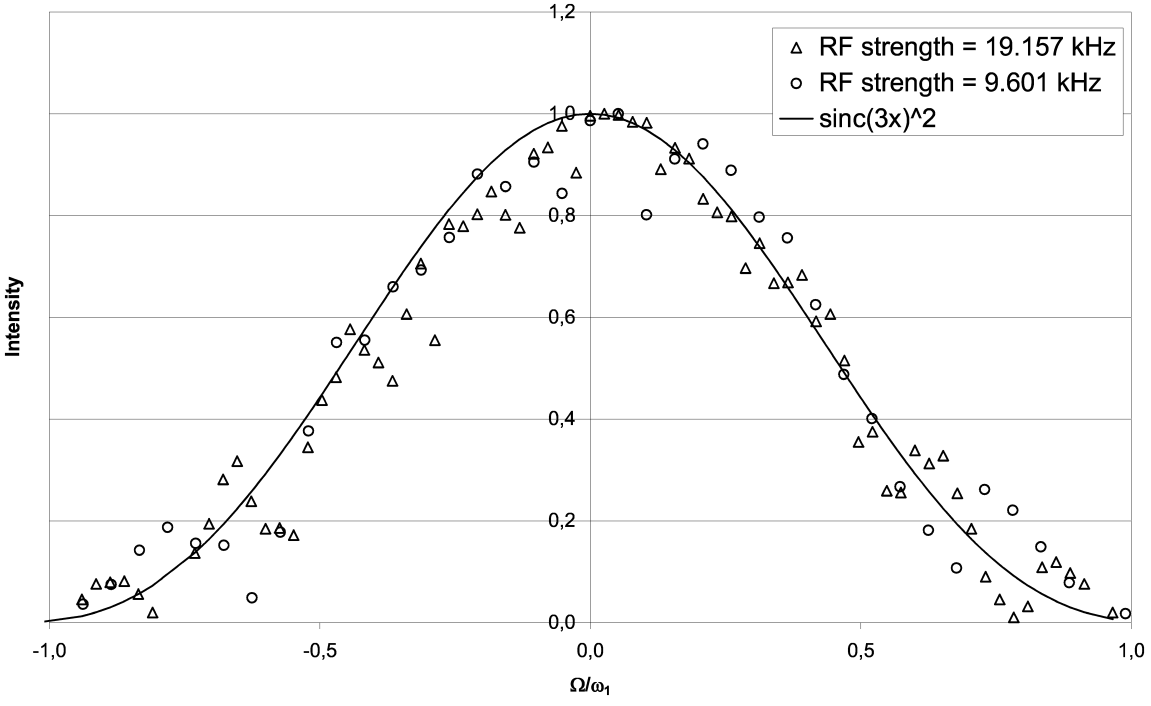

Fig. 5. The intensity (amplitude) results of 1D Q-CAHSQC experiments from methanol with two RF strengths. The offset of ^{13}C pulses was varied from 15 to −15 kHz in steps of 500 Hz. The results are plotted against relative offset Ω/ω_1, where Ω is absolute ^{13}C offset, and ω_1 ($=\gamma B_1$) is the ^{13}C RF field strength. The 1D Q-CAHSQC experiments were measured from a sample of 4% MeOH in MeOH-d4 (Bruker standard). The pulse sequence was modified by excluding t_1 evolution period, and by incorporating ^{13}C offset variation. The same acquisition parameters used in 2D experiments were mainly used for 1D experiments; apart from setting the carriage frequencies on-resonance for MeOH on ^{1}H channel. The spectral width of 3 ppm (^{1}H) was used. The offset of ^{13}C channel pulses was varied from +15 to −15 kHz about the ^{13}C resonance in steps of 500 Hz. The GARP-1 ^{13}C decoupling was omitted, and the high-field peak of ^{1}H doublet was used in order to avoid any residual ^{12}C-bound proton magnetization affect to resonance amplitude. The spectra were weighted with exponential window function prior to Fourier transform; LB was 0.3 Hz. The intensities were measured with peak picking routine.

MeOH ^{13}C resonance frequency. The experiments were executed using two RF strengths, 19.157 and 9.601 kHz, on ^{13}C channel. As can be seen from Fig. 5, the intensity behavior is similar with two different RF field strengths, when the results are plotted in function of relative offset (Ω/ω_1). With rough approximation, the offset dependency can be expressed by equation:

$$I_{^{13}C_{offset}} = (\sin c(3x))^2, \quad x \neq 0, \tag{2}$$

where x is the relative ^{13}C offset (Ω/ω_1). This equation is concluded from hypothetical sin$c$(x) type offset dependency of single 90° RF pulse. Thus, the offset dependency of two consecutive 90° RF pulses is a square of sin$c$(x) function, the factor 3 in Eq. (2) is iterated by minimizing the difference between the function and experimental results. Eq. (2) is not by any means a discreet analytical result of magnetization evolution during pulse sequence, but a robust and still sufficiently accurate tool to describe the offset dependency in any ^{13}C RF field strength; the Pearson product-moment correlation coefficient is 0.98 indicating a very good fit. Thus, the integral value can be corrected by dividing it with coefficient of Eq. (2). This approach can give quite accurate quantification results (Fig. 3). Standard deviation after coefficient correction is only 6.6%, while without correction it is 16.8%.

The second way to minimize the offset dependency, that does not involve retrospective correction of integration results, is to replace the 90° rectangle pulses by composite pulses that have a good offset compensation. The results from the composite pulse compensated Q-CAHSQC spectrum from strychnine are plotted against the results from ordinary Q-CAHSQC in Fig. 3. As can be seen, the overall performance for composite pulse compensated Q-CAHSQC is better, as standard deviation is 11.7%. For the Q-CAHSQC and Q-HSQC standard deviations were 16.8 and 17.5%, respectively. Fig. 3 shows that there is still some contribution due to the imperfection of the offset performance. In fact, the calculated resonance offset profile shown in Fig. 6 indicates that the combined M_z-profile of the composite 90° pulses used in pulse sequence shows some decay at the ends of the required chemical shift range. Thus, this approach is not applicable if the ^{13}C chemical shift range exceeds the range of ±0.3 times the available RF field strength. But if the chemical shift range lies within the aforementioned constraints, reasonable accurate results should be conceivable straight from integration results. This is indicated by standard deviation within the given limits. For composite pulse compensated Q-CAHSQC, standard deviation is 5.0%, whereas for the Q-CAHSQC and Q-HSQC the values were 9.1 and 9.4%, respectively.

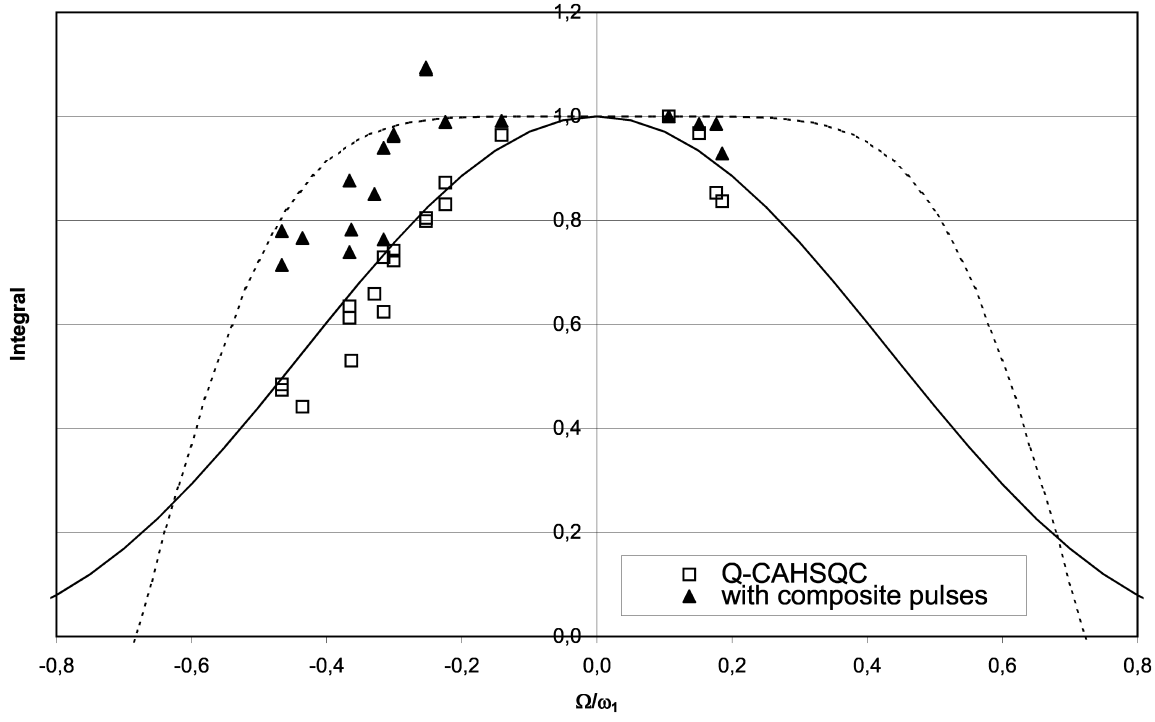

Fig. 6. Calibrated integration results of strychnine from Q-CAHSQC and composite pulse compensated Q-CAHSQC spectra plotted against relative offset Ω/ω_1, where Ω is absolute ^{13}C offset, and ω_1 ($=\gamma B_1$) is the ^{13}C RF field strength. The M_z offset profile of two consecutive composite 90° pulses used in composite pulse compensated Q-CAHSQC is shown with dotted line, and approximated offset profile given by Eq. (2) with solid line. The composite pulse offset profile was simulated with Bruker NMR-SIM Bloch module using 20 kHz for γB_1 strength.

Another method described in the literature to compensate offset deficiencies of pulse sequences is a ''global pulse sequence compensation'' reported by Levitt [19]. This approach has been successfully applied to experiments suffering from the wide chemical shift range of observed nucleus [20]. Theoretically this should give a better total offset profile when applied to carbon pulses on the subsection II of Fig. 1 compared to the method above. However, the efficiency of polarization transfer in the pulse sequence is defined by the efficiency of individual pulses as discussed in section Experimental methods, not the total offset profile. Thus, according to our tests (data not shown), this approach has no advantage over the presented composite pulse compensation.

4. Conclusions

A study of aspects affecting to the application of 2D HSQC into quantitative measurements was presented. Both theoretical and experimental results indicate, that the most important factor that can compromise quantitative results is resonance offset profile of ^{13}C channel radio frequency pulses. This dependency can be either compensated by using Q-CAHSQC in concert with coefficients to correct integration results, or when the ^{13}C chemical shift range is reasonable—about ± 0.3 times the available RF field strength—Q-CAHSQC modified with offset-tolerant composite pulses.

Acknowledgments

Finnish Institute for Verification of the Chemical Weapons Convention (VERIFIN) is acknowledged for the permission to use their facilities for this research. Special thanks to Dr. Markku Mesilaakso for providing iterated *J* coupling constants of strychnine. The Academy of Finland is acknowledged for financial support.

References

[1] M.L. Martin, G.L. Martin, J.J. Delpuech, Practical NMR Spectroscopy, Heyden, London, 1980, Chapter 9.
[2] R.K. Harris, Quantitative aspects of high-resolution solid-state nuclear magnetic resonance spectroscopy, Analyst 110 (1985) 649–655.
[3] M.R. Bendall, D.T. Pegg, D.M. Doddrell, Polarization transfer pulse sequences for two-dimensional NMR by Heisenberg vector analysis, J. Magn. Reson. 45 (1981) 8–29.
[4] M.R. Bendall, D.T. Pegg, ^{1}H–^{13}C two-dimensional chemical shift correlation spectroscopy using DEPT, J. Magn. Reson. 53 (1983) 144–148.
[5] H. Koskela, T. Väänänen, Quantitative determination of aliphatic hydrocarbon compounds by 2D NMR, Magn. Reson. Chem. 40 (2002) 705–715.
[6] T.J. Henderson, Sensitivity-enhanced quantitative ^{13}C NMR spectroscopy via cancellation of $^{1}J_{CH}$ dependence in DEPT polarization transfers, J. Am. Chem. Soc. 126 (2004) 3682–3683.
[7] G. Bodenhausen, D.J. Ruben, Natural abundance ^{15}N NMR by enhanced heteronuclear spectroscopy, Chem. Phys. Lett. 69 (1980) 185–189.
[8] S. Heikkinen, M.M. Toikka, P.T. Karhunen, I. Kilpeläinen, Quantitative 2D HSQC (Q-HSQC) via suppression of *J*-dependence of polarization transfer in NMR spectroscopy: application to wood lignin, J. Am. Chem. Soc. 125 (2003) 4362–4367.
[9] L. Mueller, P. Legault, A. Pardi, Improved RNA structure determination by detection of NOE contacts to exchange-broadened amino protons, J. Am. Chem. Soc. 117 (1995) 11043–11048.
[10] F.A.A. Mulder, C.A.E.M. Spronk, M. Slijper, R. Kaptein, R. Boelens, Improved HSQC experiments for the observation of exchange broadened signals, J. Biomol. NMR 8 (1996) 223–228.
[11] B. Luy, J.P. Marino, ^{1}H–^{31}P CPMG-correlated experiments for the assignment of nucleic acids, J. Am. Chem. Soc. 123 (2001) 11306–11307.
[12] T. Gullion, D.B. Baker, M.S. Conradi, New, compensated Carr-Purcell sequences, J. Magn. Reson. 89 (1990) 479–484.
[13] E.J. Wells, H.S. Gutowsky, NMR spin–echo trains for a coupled two-spin system, J. Chem. Phys. 43 (1965) 3414–3415.
[14] A. Allerhand, Analysis of Carr-Purcell spin–echo NMR experiments on multiple-spin systems. I: the effect of homonuclear coupling, J. Chem. Phys. 44 (1966) 1–9.
[15] R.R. Ernst, G. Bodenhausen, A. Wokaun, Principles of Nuclear Magnetic Resonance in One and Two Dimensions, Clarendon Press, Oxford, 1990, pp. 206–209.
[16] R. Freeman, J. Friedrich, X.-L. Wu, A pulse for all seasons. Fourier transform spectra without a phase gradient, J. Magn. Reson. 79 (1988) 561–567.
[17] R. Tycko, H.M. Cho, E. Schneider, A. Pines, Composite pulses without phase distortion, J. Magn. Reson. 61 (1985) 90–101.
[18] L. Braunschweiler, R.R. Ernst, Coherence transfer by isotropic mixing: application to proton correlation spectroscopy, J. Magn. Reson. 53 (1983) 521–528.
[19] M.H. Levitt, Composite Pulses, Encyclopedia of Nuclear Magnetic Resonance, vol. 2, John Wiley, New York, 1996, pp. 1396–1411.
[20] J. Bunkenbord, N.C. Nielsen, O.W. Sørensen, Doubling the sensitivity of natural abundance ^{13}C–^{13}C INADEQUATE with off-resonance compensation, Magn. Reson. Chem. 38 (2000) 58–61.